Supplemental material for

Advances in the detection of As in environmental samples using low energy X-ray fluorescence in a scanning transmission X-ray microscope: Arsenic immobilization by an Fe(II)-oxidizing freshwater bacteria

A.P. Hitchcock, M. Obst J. Wang, Y.S. Lu and T. Tyliszczak

Environmental Science & Technology

File: XRF-STXM-FeBoN-supplement.doc
Last changed: 17-Nov-11

S.1 Experimental aspects

A compact Peltier-cooled SDD system (Amptek model X-123SDD, 7 mm^2 active area) was installed in the STXM at ALS beamline 11.0.2 with the detector sufficiently close to the sample to obtain a large solid angle (estimated to be 0.5 sr) (**figure S-1a**). The windowless detector was operated at a pressure of $1x10^{-5}$ torr. For some measurements an aluminized silicon nitride membrane was used to reduce interference by scattered light from the HeNe laser used for interferometric positional control (30). We ultimately found that an aluminum metal collimator (1.5 mm diameter aperture) combined with careful positioning of the XRF detector relative to the order sorting aperture (OSA) and the sample support was sufficient to eliminate background signals from both the laser and X-rays scattered/emitted from the OSA. The detector was mounted orthogonal to the X-ray beam. The elliptically polarizing undulator (EPU) was adjusted so that the E-vector of the incident light pointed directly at the SDD, to minimize Rayleigh scattering (31). When the E-vector was intentionally oriented orthogonal to the SDD the Rayleigh scattering signal was found to be similar in magnitude to, or larger than the strongest X-ray fluorescence from the sample (**Fig. S-1b**). We confirmed that the elastic scattering signal made negligible contribution to the results, even with photon energies within the energy of the As Lα XRF peak (see **Fig. S-2**).

In order to verify that the elastic scattering signal is not significantly contributing to the As Lα yield map, XRF maps were recorded with 1400 eV photon energy where there is only a small overlap of the As Lα and elastic peaks so that it is easy to obtain independent maps of these two signals. **Figure S-2a** is the XRF spectra recorded from on and off the sample in the regions indicated by the green circle and red rectangle respectively. **Figure S-2b** is the As map and **Figure S-2c** is the signal from the elastic scattering, which is nearly featureless with an intensity level about 10% of that of the As Lα signal.

S-2 Results

An advantage of the combination of transmission and XRF detection is that the conventional transmission mode can be used for quantitative speciation and mapping of major components using NEXAFS image sequences (13), while the XRF and XRF-yield NEXAFS maps provide details of the minor and trace elements. **Figure S-3(a-c)** presents component maps for protein, polysaccharide and lipid derived from a stack fit analysis of a C 1s image sequence (37, 38) recorded in the sample area examined in Figure 1. **Figure S-3d** presents the map of the constant signal from the stack fit of the C 1s image sequence, which corresponds to the strong iron component as well as other non-organic species present. **Figure S-4a** is a color composite of the maps of protein, polysaccharide and lipid components. **Figure 4b** is a color composite of the Fe(III) map ($OD_{710} - OD_{704}$) and the pre-Fe edge image at 704 eV, which is dominated by the O 1s continuum of the Fe-oxide and biological components, and the C 1s continuum of the biological components. These conventional STXM results provide a helpful background to discuss the As spatial distributions determined by XRF and XRF-NEXAFS mapping.

Figure S5 presents the average XRF spectrum (Fig. S-5a), the OD and total fluorescence maps as well as XRF maps for all detected elements (C, N, O, Fe, Cu, Na and {As&Mg}) measured using 1360 eV incident photon energy. Note that the level of Mg relative to As is very low and the Mg distribution is similar to that for As, as indicated by the Mg and As maps derived from XRF-yield image sequences over both the Mg 1s and As 2p edges (see Figure 3 of reference 14). The total fluorescence yield image (Fig S-5j) is similar but not identical to the OD image from

the transmission signal (Fig. S-5b). The strongest X-ray fluorescence signals are from C, O, Fe and the {As&Mg} signals. Weak Cu and Na signals are also detected. The N map is dominated by the signal from the exposed Si_3N_4 substrate. Systematically there is higher XRF intensity at the right hand side of the cell and deposits, which is the side closest to the SDD. The images generated from the low energy carbon, nitrogen and oxygen Kα fluorescence signals are shaded due to absorption of these soft X-ray fluorescent photons from parts of the sample closer to the detector (a very shallow exit angle (15^o) was used – see Figure S-1a).

Figure S-6 presents As 2p X-ray absorption spectra detected by As Lα XRF yield extracted from 3 different regions of the image sequence for which the XRF-yield spectra are presented in Fig. 4. The inset image indicates the areas from which the signals for cells (green), debris off cells (blue) and background (red) were averaged. The signal from the debris is about 60% that of the signal from directly on the cells, while the signal off the biofilm is 30-50 times smaller. Note that the As 2p spectral shape is that characteristic of As(V) [35] in all regions.

Figure S-7a shows the As map derived from the XRF-yield NEXAFS image sequence (fit to the As 2p absorption spectrum and a constant) while **Figure S-7b** presents a color composite of the Fe signal (red, Fe Lα XRF image averaged over the whole image sequence), the As Lα signal (blue, see Fig. S-7a) and the cell signal (green, from the average pre-edge image which visualizes the cells better than the C Kα signal). It is interesting to compare the STXM-XRF maps with elemental maps obtained by state-of-the-art energy-dispersive X-ray fluorescence mapping in a scanning electron microscope (SEM). **Figure S-7c** shows the As map from the As Kα XRF recorded from area A (identical to that in Figs. 7a,b) measured in a Tescan Vega-2 SEM, using a large area SDD detector (Oxford Xmax80) with a comparable integration time to that used for the XRF-yield NEXAFS image sequence. **Figure S-7d** is a color composite of the Fe Kα, C Kα and As Kα SEM-XRF signals. Similar acquisition times were used for the SEM-EDX and synchrotron XRF measurements. In general there is good agreement between the SEM-EDX and STXM-XRF results. The intensity of each color in the composite maps has been rescaled so Fig. S-7b and S-7d compare the relative spatial positioning of the three components and not their relative amounts. Some differences in relative amounts are to be expected since the relative

yields for the different X-ray emission lines (Lα and Kα) differ and the 20 keV electron beam in the SEM does not penetrate as far into the sample as the soft X-rays.

Figure S-8 presents further details of the As/Fe distributions presented in figure 5. In particular histograms of the As / Fe ratios [counts/counts] are presented in three selected regions (locations are color coded in the associated image). This shows clearly that, for the signals associated with this type 3 cell, the amount of As is largest in the outer extracellular precipitates and smallest in the former cytoplasm.

Figure S-9 presents line profiles of the As/Fe ratio and the OD signals across the stage 3 cell for which the As/Fe distributions are presented in figure 5. The enhancement of the As relative to Fe at the outer boundary of the cell is clear. The elevated As/Fe signal to the right side at ~ 1 micron from the centre of the cell is from a small piece of extracellular precipitate that has spalled off this cell (see arrows in Figs S-9a-c).

Figure Captions

Figure S-1 (a) Photograph of the silicon drift detector (SDD, Amptek) for energy dispersive X-ray fluorescence (XRF) spectrometry implemented in the scanning transmission X-ray microscope (STXM) at beamline 11.0.2 at the Advanced Light Source. **(b)** X-ray fluorescence spectra recorded from an As (V) hot spot found in a *Acidovorax* sp. strain BoFeN1 sample. Spectra were recorded with both horizontal E-vector (pointing towards the SDD), and vertical E-vector. The elastic (Rayleigh) scattering is minimized when the linear polarization is adjusted so the E-vector points at the XRF detector. (ALS)

Figure S-2 (subset of area B) **(a)** X-ray fluorescence spectra from an As-rich hot spot (circle) and from an area of lightly covered Si_3N_4 window (rectangle) recorded with the XGLab SDD at CLS-STXM using 1400 eV incident photon energy and a polarization such that the E-vector pointed at the SDD. **(b)** Average image for the XRF signal from 1200 – 1360 eV, corresponding to the As Lα (and some Mg Kα) signal. **(c)** Average image for XRF signal from 1380 – 1500 eV, corresponding to elastic scattering. (CLS)

Figure S-3 (area A) Component maps for **(a)** protein, **(b)** polysaccharide, **(c)** lipid, and **(d)** non-carbon (constant of stack fit) of the *Acidovorax* sp. strain BoFeN1 sample derived from a C 1s image sequence (280 – 320 eV, 66 energies, 1 ms/pixel) using transmission detection. The grayscale limits for the protein, polysaccharide and lipid maps are the thickness in nm, while the grayscale for the constant map is the mean OD in the C 1s region. (ALS)

Figure S-4 (area A) **(a)** Color coded composite of the protein (red), polysaccharide (green) and lipid (blue) signals of the *Acidovorax* sp. strain BoFeN1 sample derived from a C 1s image sequence (280 – 320 eV, 66 energies) using transmission detection. Each component map is independently rescaled. The individual component maps are presented in the supplemental material. **(b)** Color coded composite of the Fe(III) signal ($OD_{710} - OD_{704}$, blue) and the pre-Fe signal (green). (ALS)

Figure S-5 (subset of area B) **(a)** X-ray fluorescence spectrum, recorded with XGLab SDD with 1700 eV incident photon energy, averaged over all pixels of an X-ray fluorescence map (6 s/pixel, 40 x 33 pixels). **(b**) optical density map (from transmission), **(c-i)** Elemental maps from integration of the peaks in the X-ray fluorescence signal; and **(j)** total fluorescence yield map, recorded for 27x34 pixels, with 2.5 s/pixel using 1360 eV incident photon energy. The numbers indicate the minimum and maximum counts in each map. (CLS)

Figure S-6 (area A) X-ray absorption spectra detected by As Lα yield for cells (green), Fe-rich debris off cells (blue) and background (red). The signal for the background has been multiplied by 10. (ALS)

Figure S-7 (area A) **(a)** As map derived from the X-ray absorption signal recorded with As Lα XRF-yield in the As 2p region. The image sequence was fit to the mean As 2p spectrum plus a constant. The yellow rectangle indicates the area for which more detailed XRF maps are presented in figure 8. **(b)** Color coded composite of the Fe Lα (red) and As Lα (blue) maps derived from the XRF-yield sequence integrated over the incident photon energy range of 1315-1380 eV, combined with an image mainly of the cells (green) which is the average of the pre-As 2p signal in the OD image derived from the transmission signal. Dwell time was 500 ms/pixel and the images are 40 x 40 pixels (0.25 μm step size) (ALS) **(c)** As map from the same area recorded using energy dispersive X-ray (EDX) detection in an SEM (Tescan Vega-2 with Oxford Xmax80 detector). The SEM-EDX data was acquired with 20 keV primary electrons, 2s/pixel, 78 x 83 pixels. A background region of the same energy width adjacent to the As Kα and Fe Kα signals was subtracted to obtain the net signal. **(d)** color coded composite of Fe Kα (red), O Kα (green) and As Kα (blue) SEM-EDX signals.

Figure S-8 (subset of area A) Histograms of the As / Fe ratios [counts/counts] in three selected regions of the area examined in detail in figure 8. Green is the area of former cytoplasm; Red is the extracellular precipitates in close association with the cell; Blue is the outer extracellular precipitates. The mean values of the As / Fe ratio [counts/counts] are 0.77, 1.09 and 1.46 respectively. (ALS)

Figure S-9 (subset of area A) **(a)** Optical density image of a stage 3 cell (see Figure 8a). **(b)** As/Fe ratio map derived from the XRF measurements. In both (a) and (b) the dotted rectangle indicates the area over which line profiles (running from bottom left to upper right) were averaged. **(c)** Line profiles of the OD (green, which defines the morphology) and the As/F ratio (red) over the areas indicated in Figures S-6a and S-66b. Note that the vertical stage 1 cell (to the left) shows negligible As signal. (ALS)

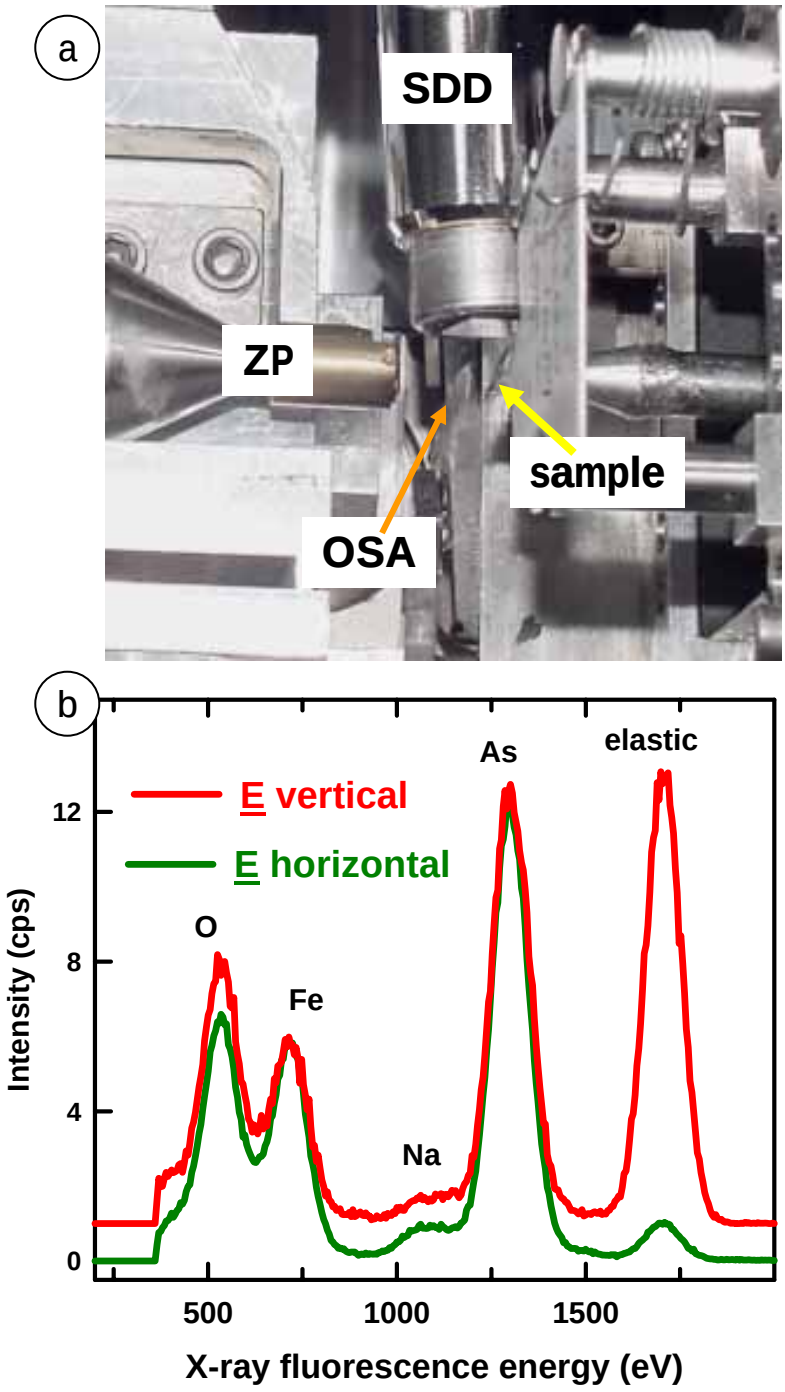
a
SDD
ZP
sample
OSA
b
E vertical
E horizontal
O
Fe
Na
As
elastic
Intensity (cps)
0
4
8
12
500
1000
1500
X-ray fluorescence energy (eV)

Fig. S-1

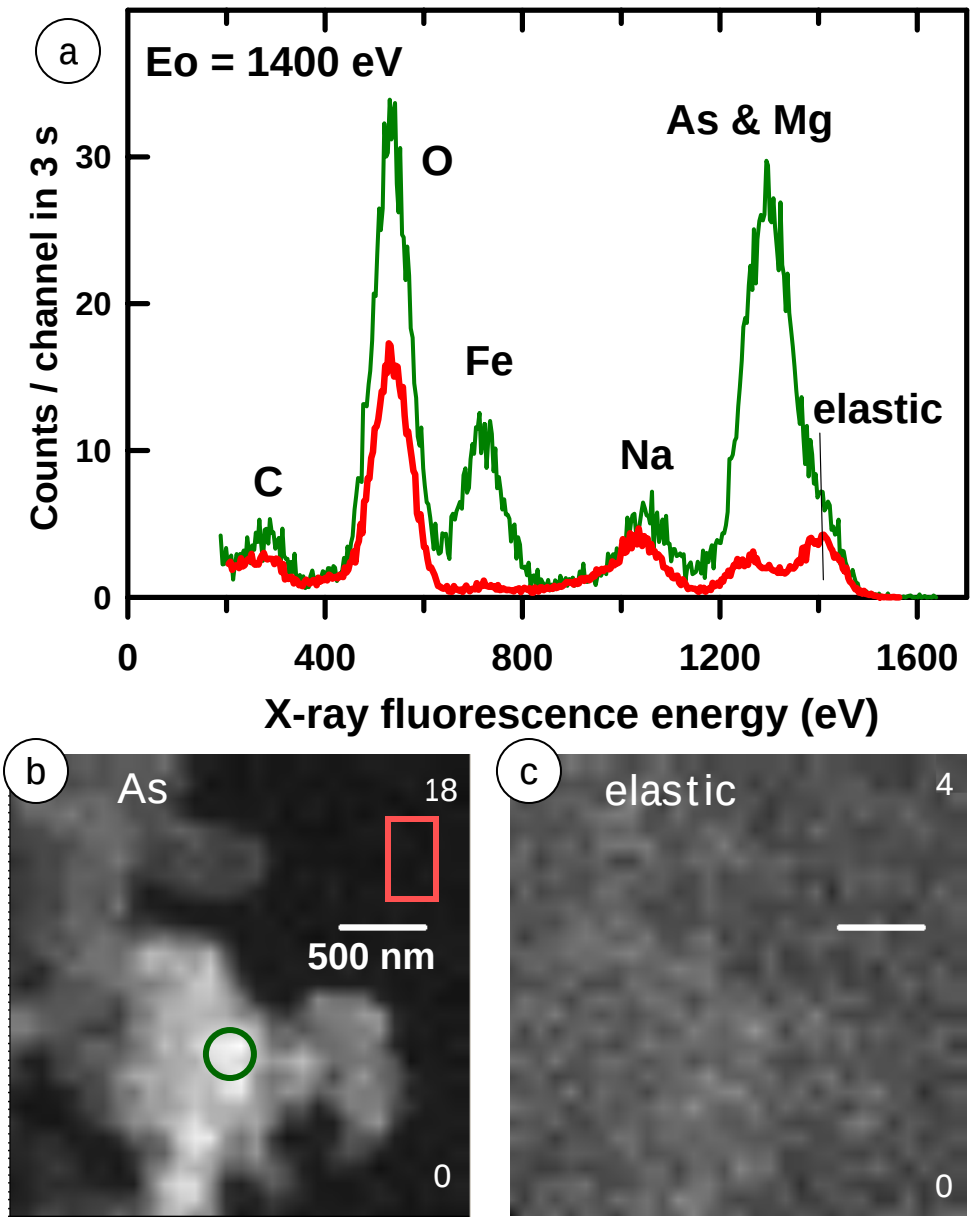
a
Eo = 1400 eV
Counts / channel in 3 s
30
20
10
0
C
O
Fe
Na
As & Mg
elastic
0
400
800
1200
1600
X-ray fluorescence energy (eV)
b
As
18
500 nm
0
c
elastic
4
0

Fig. S-2

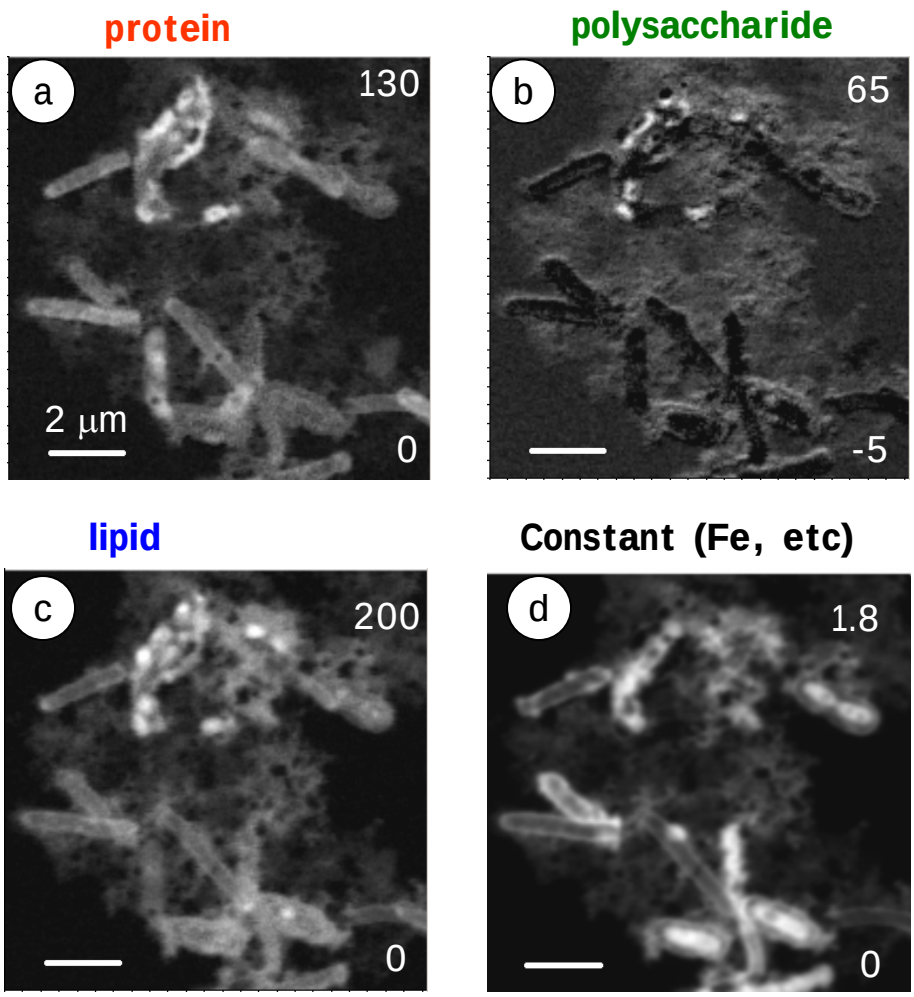
protein
a
130
2 μm
0
polysaccharide
b
65
-5
lipid
c
200
0
Constant (Fe, etc)
d
1.8
0

Fig. S-3

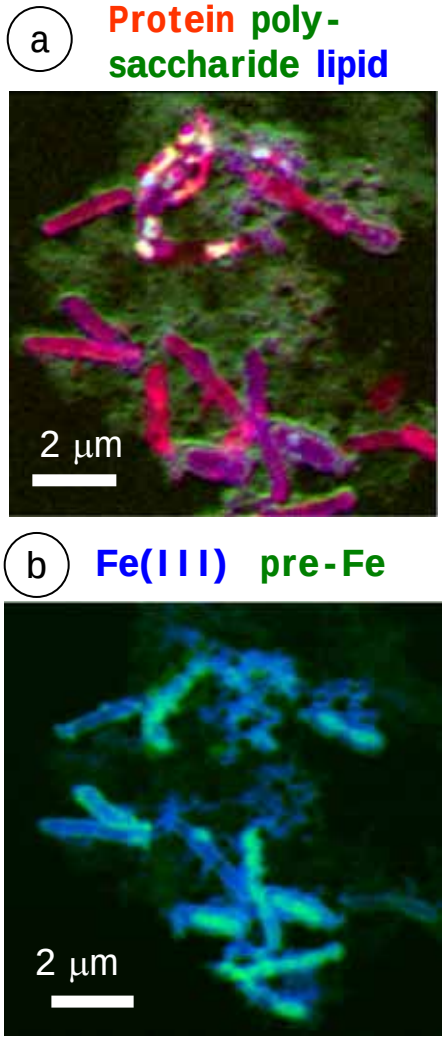

Fig. S-4

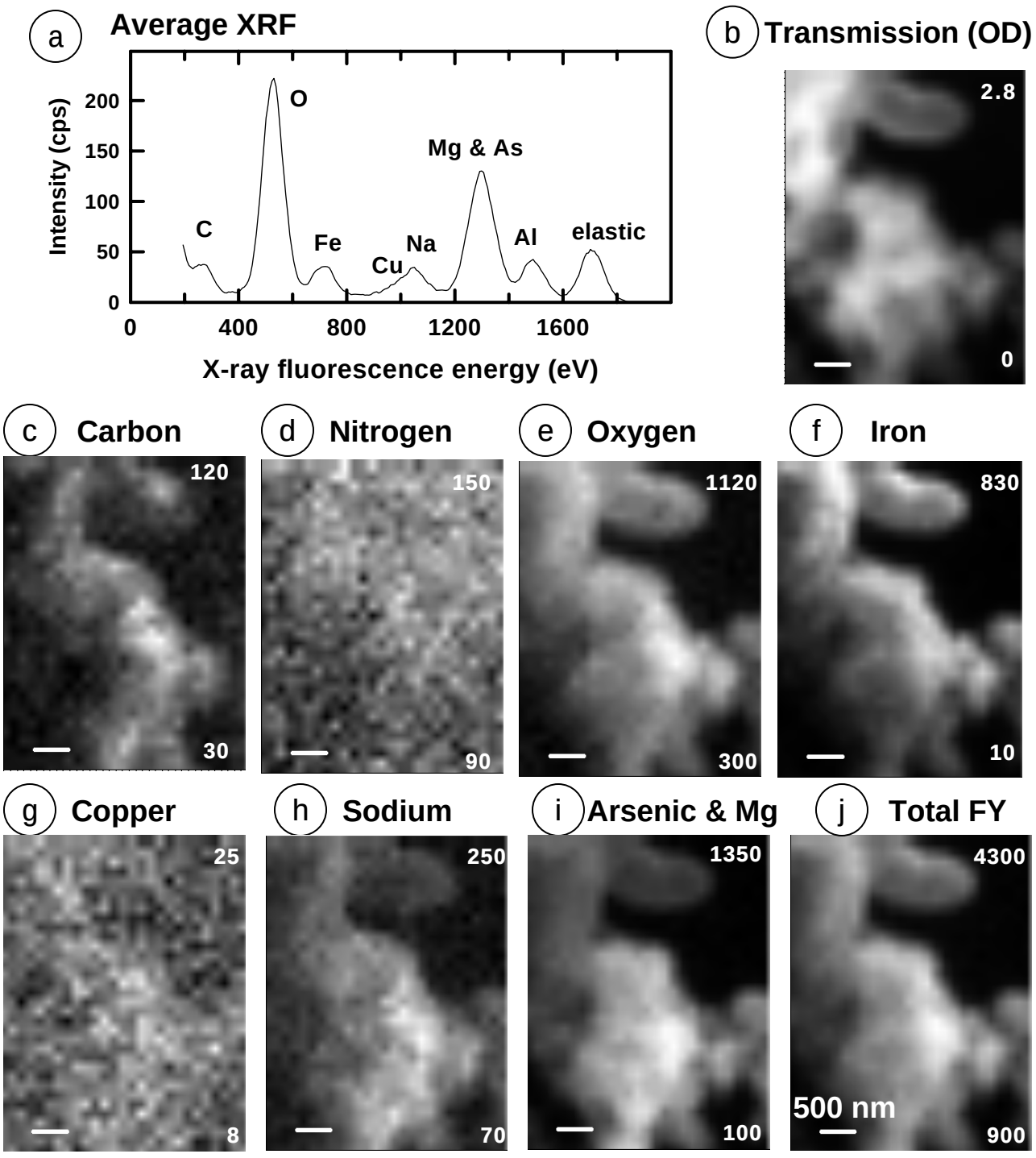
a
Average XRF
Intensity (cps)
200
150
100
50
0
0
400
800
1200
1600
X-ray fluorescence energy (eV)
C
O
Fe
Cu
Na
Mg & As
Al
elastic
b
Transmission (OD)
2.8
0
c
Carbon
120
30
d
Nitrogen
150
90
e
Oxygen
1120
300
f
Iron
830
10
g
Copper
25
8
h
Sodium
250
70
i
Arsenic & Mg
1350
100
j
Total FY
4300
500 nm
900

Fig. S-5

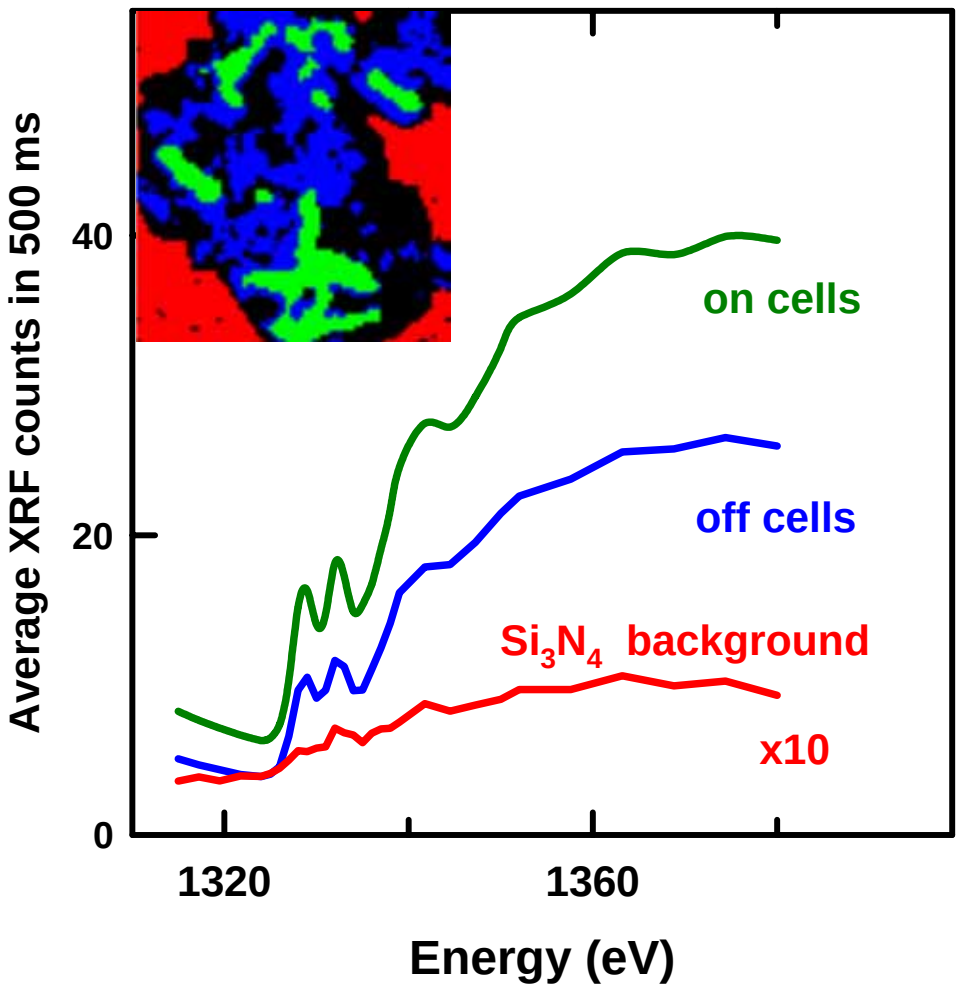
Average XRF counts in 500 ms
40
20
0
1320
1360
Energy (eV)
on cells
off cells
Si3N4 background
x10

Fig. S-6

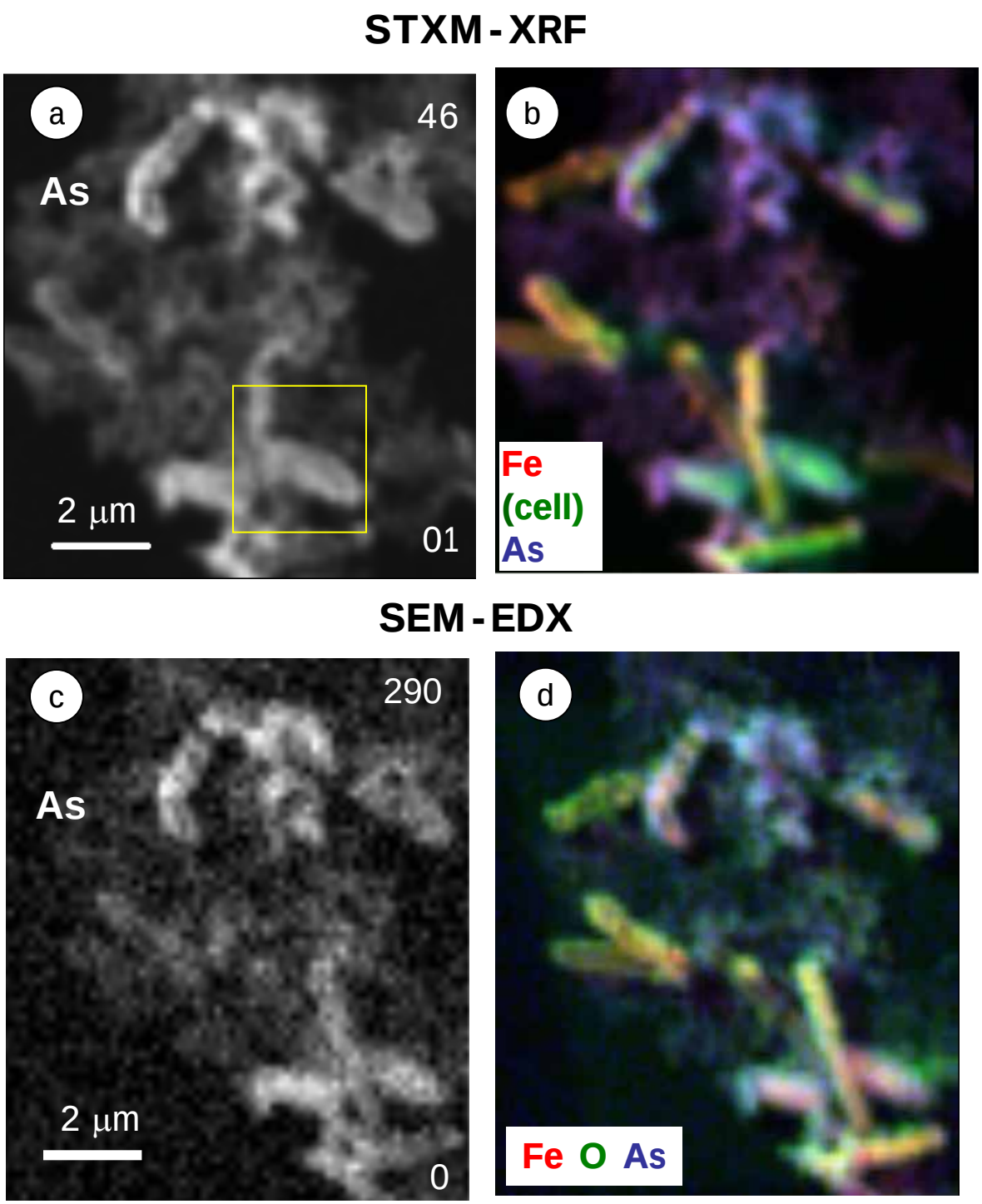

Fig. S-7

Background: linear absorbance image (OD). The numbers indicate the As/Fe ratios of the respective areas.

green: area of former cytoplasm
red: extracellular precipitates in close association with the cell
blue: outer extracellular precipitates

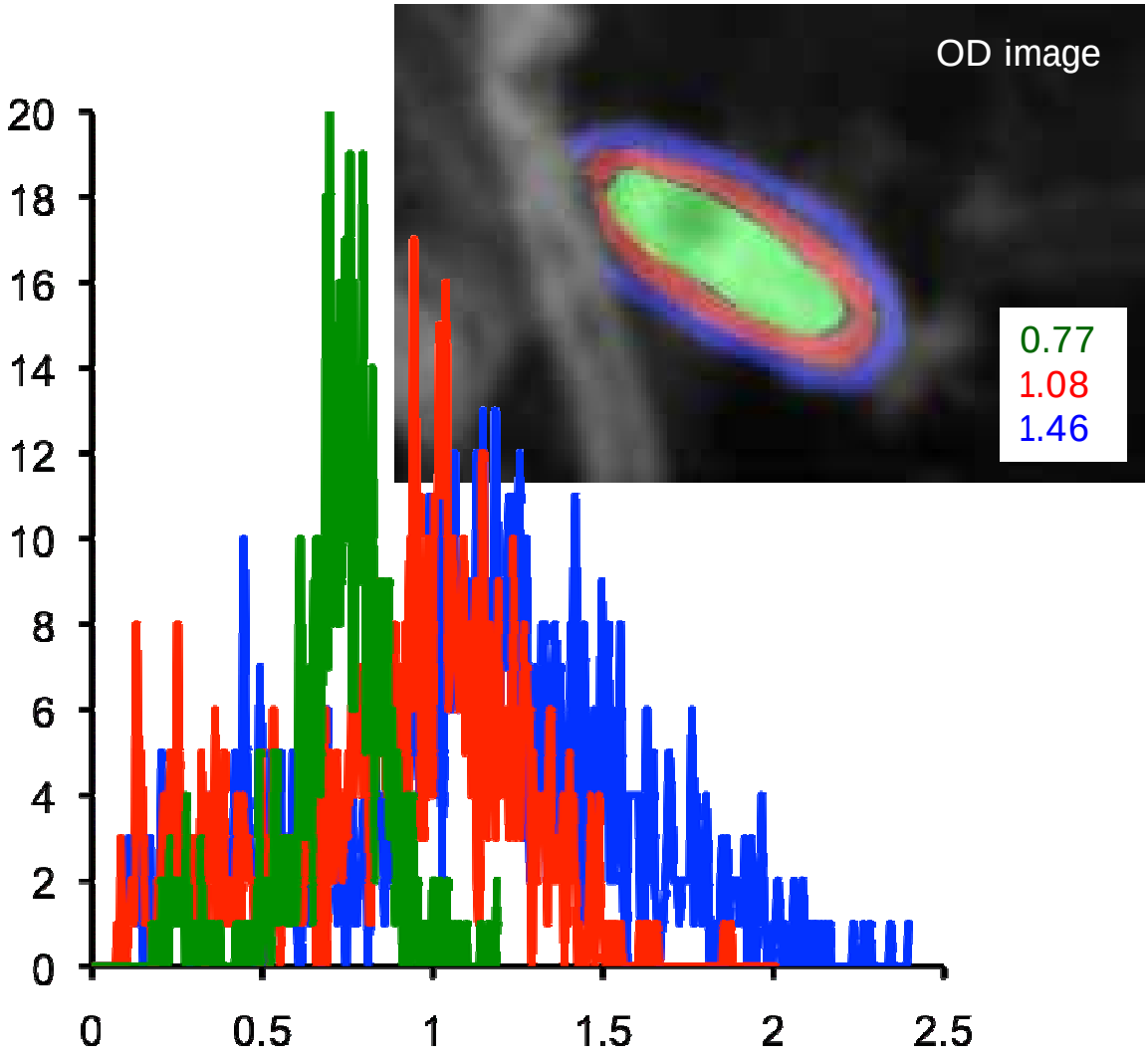

Fig. S-8

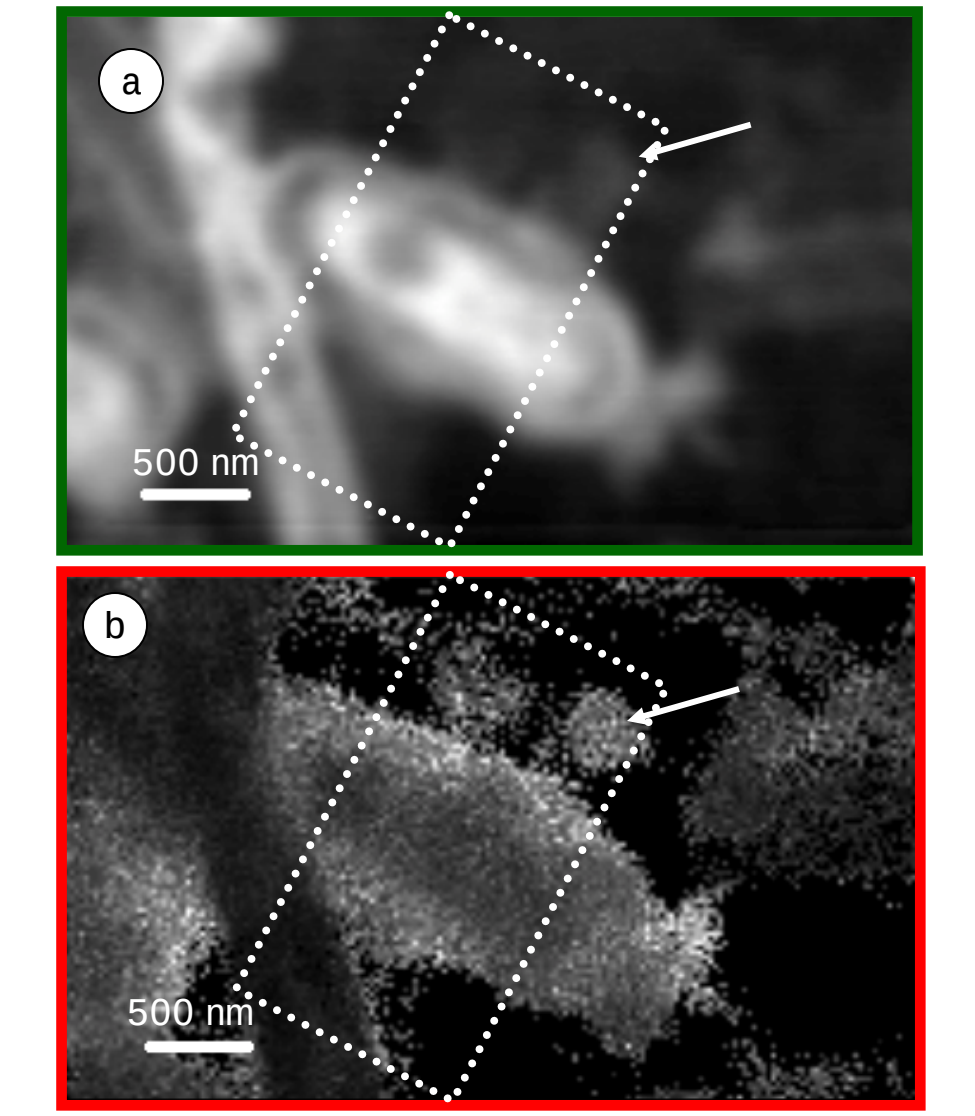
a
500 nm
b
500 nm
c
As/Fe ratio is enriched towards the outside of the precipitates
OD
ratio As/Fe [counts/counts]
linear absorbance [OD]
As/Fe ratio [counts/counts]
distance from cell axis [µm]
1.0
0.5
0.0
2
1.5
1
0.5
0
-2
-1
0
1
2

Fig S-9